Reverse Time Migration of up and down going signal for ocean bottom data

Mandy Wong, Biondo L. Biondi, and Shuki Ronen

ABSTRACT

We present the results of reverse time migration (RTM) on ocean-bottom data as a precursor to applying reverse time migration and inversion of multi-component ocean-bottom data using the two-way acoustic wave-equation. We propose a joint-inversion scheme that constructively combines up- and down-going migration results and removes spurious artifacts in the final image. Reverse time migration of up-going data gives stronger reflector amplitude and weaker artifacts than migration of down-going data; however, due to mirror-imaging, the area of sub-surface illumination is narrower when using up-going energy. In addition, we observe that a new class of artifacts is present due to RTM injection of receiver wavefields with the ocean bottom geometry.

INTRODUCTION

Reverse time migration (RTM) is a method of choice for imaging complex structure due to its ability to image steep reflectors (Baysal et al., 1983; Whitmore, 1983; Etgen, 1986). Despite its computational cost and sensitivity to the background velocity model, RTM has evolved from poststack migration to prestack migration using single component data acquired with the traditional streamer geometry. However, conventional streamers acquisition has significant limitations. One limitation is that production and drilling rigs interfere with the survey geometry. Such obstructions cause large gaps in the coverage of streamer surveys. Undershooting such obstructions with a separate source vessel is an imperfect solution because of the varying offset and azimuth distribution of such undershoots. These limitations foster a growing demand for ocean bottom seismometers (OBS). OBS data acquisition is an alternate approach in which seismometers are placed on the seafloor and shots are fired at the ocean surface. Therefore, OBS surveys are less sensitive to structural obstacles. OBS have other advantages including: full azimuth coverage, multi-component data, and potentially improved repeatability. Full azimuth coverage improves imaging and demultiple processing under complex overburden. Multi-component data enables better demultiple processing, or even imaging with multiples. Moreover, recording of shear waves contains additional information about the lithology and fractures and are less sensitive than P waves to gas clouds. These advantages often justify the additional cost of acquiring OBS data.

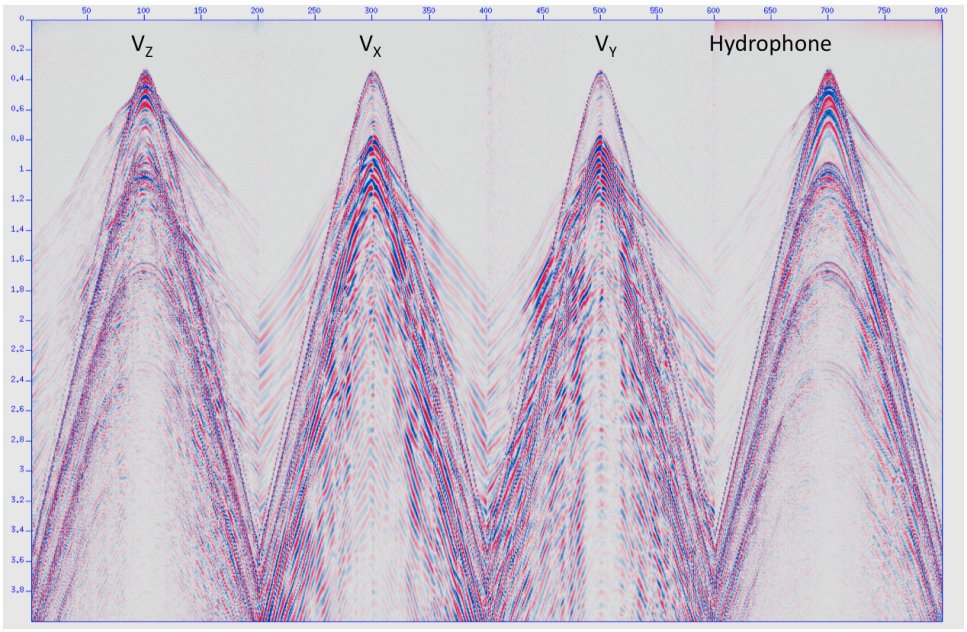

Figure 1: Four component (4C) common receiver gather for a single shot line. **[NR]**

The ultimate goal of our research is to develop a better way to image OBS data and to refine the art of processing OBS data. The most significant difference is that OBS data are multi-components: pressure P, and the three components, X, Y, Z, of the particle velocity or acceleration. Figure 1 shows a common receiver gather of a single shot line in a typical ocean bottom acquisition. From Figure 1, we can see that both pressure (P) and shear (S) waves are recorded. A natural approach is to use elastic modeling in the migration process. Indeed, Yan and Sava (2008) has proposed a way to perform isotropic elastic reverse time migration in the angle-domain. Such a scheme, although feasible, is still computationally expensive and the dependency on both P and S velocity model can be challenging.

At this stage, we focus on P wave imaging. The hydrophone records both up- and down-going pressure waves. The additional information from the OBS geophone's Z velocity measurement includes a polarity flip between up- and down-going waves. This enables separation of the up- and the down-going waves. Accounting for instrument gain, coupling to the seabed, and the fact that pressure is the acoustic impedance times the particle velocity, we can write:

$$\begin{aligned} P &= \text{Up} + \text{Down}, \\ Z &= \text{Up} - \text{Down}. \end{aligned} \tag{1}$$

Therefore, up- and down-going data at the receiver can be obtained as shown,

$$\text{Up} = \frac{P+Z}{2},$$
$$\text{Down} = \frac{P-Z}{2}. \tag{2}$$

Equation 2 is often refered as *PZ summation* (White, 1965; Barr and Sanders, 1989; Amundsen, 1993). The advantage of turning P and Z data into up- and down-going data is that primary reflection events are contained solely in the up-going data. Therefore, a "conventional" migration can be performed on the cleaner up-going data. Recent work by Dash et al. (2009) suggested that the down-going waves should also be processed. Imaging the down-going waves is known as mirror imaging (Ebrom et al., 2000). We seek to incorporate the information in migrating with up-going data and migrating with down-going data by using a joint-inversion scheme as illustrated in Figure 2 and Figure 3.

After velocity analysis, migration is the process that estimates the earth reflectivity for given data and velocity model. With the velocity as the parameter space, migration is a linear operator (Figure 2(a)). Similarly, with the same parameter and model space, modeling is a linear operator (Figure 2(b)) and can be inverted. Figure 2(c) describes the concept of linear inversion. Migration and stacking is the adjoint of modeling. Sometimes the adjoint is a very good approximation to the inverse. Ideally, a good adjoint (migration) operator should be as close to the inverse of modeling as possible.

For single-component (acoustic) data, imaging with migration or with inversion are common. For multi-component ocean bottom data, applying the corresponding concept would require the use of elastic wave-equation either in migration or in inversion (Figure 2(d)). Elastic modeling is costly and the dependency on both P and S velocity models is problematic. On the other hand acoustic modeling is less costly and does not depend on shear velocity. We limit our ambition to acoustic waves and use hydrophone and vertical component of geophone measurements to image with both the primaries and the multiples signal. We illustrate this method in Figure 3. P and Z data can be converted into up- and down-going data with PZ summation, Equation 2. Up- and down-going data can be converted into over/under data, which are pressure waves sampled at two depth levels. Effectively, we can transform from P and Z data to up- and down-going data, and finally to over/under data. This allows us to perform inversion in the acoustic regime.

It is worth mentioning that our joint inversion scheme can be applied to the processing of dual-sensor streamer data. The P and Z measurements of dual-sensor data can be conveniently combined to produce up- and down-going data using PZ summation and subsequently be used for joint-inversion imaging. The two advantages with this procedure for dual sensor data are (1) the repairing of attenuated signal at the notch frequencies and (2) the improved image from the additional information provided by the mirror signal (receiver ghost).

This is a progress report to apply joint inversion of up- and down-signal described in

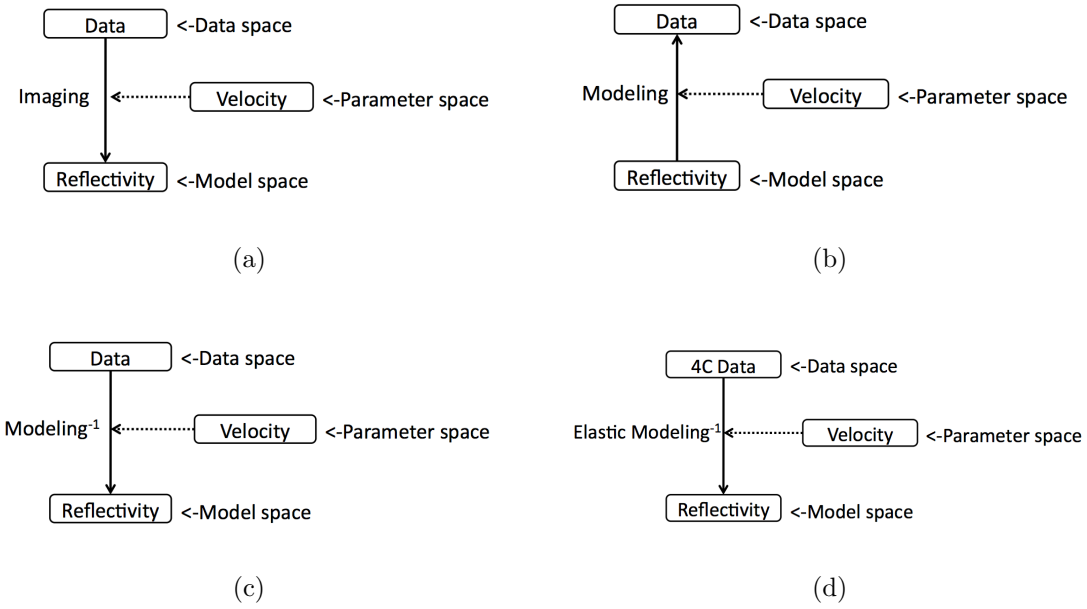

Figure 2: (a) The processing flow of imaging with reflectivity, also known as migration. (b) The flow of modelling, which creating synthetic data from reflecitivity and velocity. (c) The flow of inversion, which is linear if the model space is reflectivity and the velocity is in the parameter space. (d) The flow of elastic inversion. [**NR**]

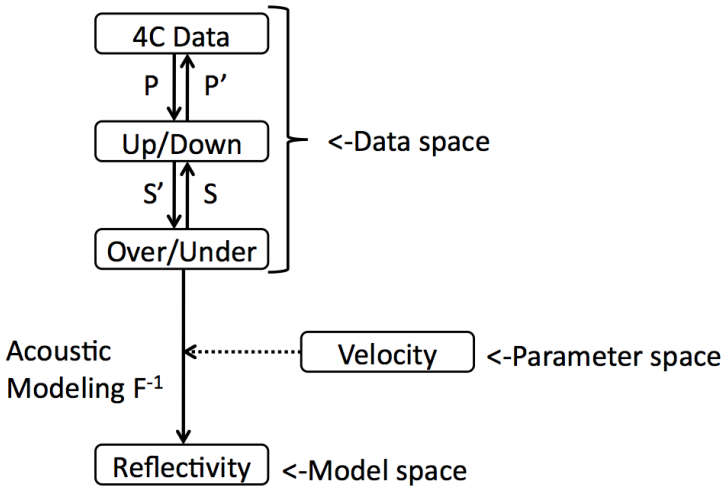

Figure 3: Acoustic inversion of multi-component data using only the P waves. Preprocessing of the 4C data to over/under enables us to use acoustic- instead of elastic-modeling. [**NR**]

Wong et al. (2009). We apply reverse time migration to synthetic ocean bottom data to compare the migration result using either the up-going or the down-going signal. While OBS measure the pressure and shear waves, we limit our synthetic study to acoustic data only. To avoid using elastic modeling to synthesize multi-component ocean bottom data, we generate acoustic up- and down-going ocean bottom recording in two steps. First, two-way acoustic wave-equation is used to generate data at two different depths level, called the over/under data, near the seabed. Then an up-down separation operator, $\mathbf{S}$, is applied to produce our desired up- and down-going ocean bottom data.

We found that while migrating the up-going data gives strong reflector amplitudes and weak artifacts, its area of sub-surface illumination is narrower than migrating with down-going signal. We also found that there are additional RTM artifacts because of the recorded waves injection at the ocean bottom. This new class of artifacts does not exist with the traditional streamer geometry.

The rest of the paper is organized as follows. We first explain our method of constructing the RTM operator and the up-down separation operator. Next, we present the results of migrating with the up-going wave only, down-going wave only, and the total signal. A discussion on the types of artifacts follows. Finally, we propose a way to eliminate ocean bottom RTM artifacts, as well as combining up- and down-going migration results using joint inversion, which will be the focus of future research.

THE RTM AND THE UP-DOWN SEPARATION OPERATORS

The RTM operator

Since there are many different ways to implement reverse time migration, we must specify how we construct our RTM operator. Our model space is the reflectivity of the subsurface. It is computed by cross-correlating the source wavefield with the receiver wavefield injected backward in time,

$$m(\mathbf{x}) = \sum_{\mathbf{s}} \sum_{t} u_s(\mathbf{x}, t, \mathbf{s}) u_r(\mathbf{x}, t, \mathbf{s}), \tag{3}$$

where $\mathbf{s}$ marks the location of the source, t is the time, $\mathbf{x}$ represents a point in the sub-surface, $m(\mathbf{x})$ is the reflectivity of the sub-surface, and $u_s(\mathbf{x}, t, \mathbf{s})$ and $u_r(\mathbf{x}, t, \mathbf{s})$ are the source and receiver wavefields at location $\mathbf{x}$, time t, and shot location $\mathbf{s}$. Our reverse time migration is set up so that $u_s(\mathbf{x}, t, \mathbf{s})$ and $u_r(\mathbf{x}, t, \mathbf{s})$ are computed using a background velocity model, $V_o(\mathbf{x})$ and the constant-density acoustic wave equation:

$$\frac{1}{V_o^2} \frac{d^2 u}{dt^2} = \nabla^2 u. \tag{4}$$

In our finite differencing scheme, we approximate the Laplacian to fourth order in space and the time derivative to second order in time. Note that in this study, we only migrate with the correct velocity. The correct velocity is smoothed to avoid spurious cross-correlation artifacts.

For ocean-bottom data, the receiver ghost reflection is very valuable, because when applied with mirror imaging, it produces better sub-surface illumination than the primary event. This claim will be apparent from later results. To create overlapping of the receiver ghost for ocean bottom RTM, we must have a reflecting top boundary.

The up-down separation operator

The derivation for decomposing over/under pressure waves into up-going and down-going signals is best done in the Fourier domain. For a thorough review of this method, please refer to Sonneland et al. (1986). Denote $P_1(\omega, k_x)$ and $P_2(\omega, k_x)$ to be the Fourier-transformed measurements of compressional waves at depths z_1 (over) and z_2 (under). Theoretically, $P_1(\omega, k_x)$ is a sum of the up-going $U_1(\omega, k_x)$ and down-going $D_1(\omega, k_x)$ components. Likewise for $P_2(\omega, k_x)$:

$$\begin{aligned} P_1(\omega, k_x) &= U_1(\omega, k_x) + D_1(\omega, k_x), \\ P_2(\omega, k_x) &= U_2(\omega, k_x) + D_2(\omega, k_x). \end{aligned} \tag{5}$$

Down-going waves arrive at the under array (D_2) before the over (D_1) array. Therefore, shifting D_2 forward in time would match the signal D_1. Similarly, up-going waves visit the over array first. Therefore, shifting U_1 forward in time would match the signal U_2. This relationship is equivalent to a phase-shift in the Fourier domain:

$$\begin{aligned} e^{ik_z \Delta z} D_2 &= D_1, \\ U_2 &= e^{ik_z \Delta z} U_1, \end{aligned} \tag{6}$$

where $\Delta z = z_2 - z_1$, and k_z is the usual dispersion relation. Finally, substituting equation 6 into equation 5 yields the formula for the up-going and down-going waves at the receivers:

$$\begin{aligned} U_2 &= \frac{P_2 - e^{ik_z \Delta z} P_1}{1 - e^{2ik_z \Delta z}}, \\ D_2 &= \frac{e^{ik_z \Delta z} P_1 - e^{2ik_z \Delta z} P_2}{1 - e^{2ik_z \Delta z}}. \end{aligned} \tag{7}$$

Over/under acquisition is used to eliminate receiver ghosting and water reverberation. Although over/under arrays are rarely placed on the sea floor in real seismic surveys,

this technique allows easy generation of up-going and down-going waves at the sea bottom for synthetic examples or modeling. For the remaining of this paper, we will denote the operation that separates over/under data into up-down data in equation 7 as $\mathbf{S}$.

SYNTHETIC OCEAN-BOTTOM DATA

Originally, field ocean-bottom data consists of two measurements, the pressure and the shear waves. However, we limit our synthetic study by using the acoustic wave equation instead of the elastic wave equation. Instead of converting the P and Z measurements into up- and down-going data, we use the constant density, two-way acoustic wave equation to first generate over/under data, which are measured at two depth levels near the ocean bottom. Next, we convert the over/under data into up-down data using the separation operator $\mathbf{S}$ described in the last section. We use a very simple one-reflector problem. Figure 4(a) shows the velocity model used to generate the synthetic over-under data.

One shot is fired at zero depth and $x = 5500$ m. Two lines of receivers are placed at 480 m and 500 m depth and span from $x = 0$ m to $x = 14000$ m with a 10 m spacing. The receiver signals are shown in Figure 4(b). The first signal that arrives in time is the direct arrival, which propagates from the source directly downward to the receivers. The second signal is our primary reflection that bounces off the reflector at 800 m depth and returns to the receiver going upward. The third signal is the receiver ghost. Figure 4(c) and Figure 4(d) show a close up of the direct arrival and primary reflection of the over and the under data collected. Notice that the direct wave arrives sooner in figure 4(c) than in figure 4(d), because the direct arrival is down-going. Similarly, the up-going primary reflection arrives sooner in Figure 4(d) than in Figure 4(c).

RTM ON OCEAN-BOTTOM DATA

In our RTM scheme, we perform migration by injecting over-under data into the finite difference grid. Figure 5(a) shows the resulting reflectivity after injecting the over signal at 480m depth and under signal at 500 m depth. As expected from the original velocity model displayed in Figure 4(a), there is a reflector below the 800 m depth. In addition, there are also two weaker coherent artifacts at 1200 m and 1300 m depth.

We also migrate with only the up-going and only the down-going signal. This can be accomplished using the adjoint of the up-down separation operator $\mathbf{S}'$ and zeroing the appropriate data component in the up-down space. Let d_o and d_u be the over and under data synthesized as described in the last section. To filter out the down-going energy in d_o and d_u, we can zero the down-going data in the up-down data space before applying the adjoint separation operator $\mathbf{S}'$ as shown below:

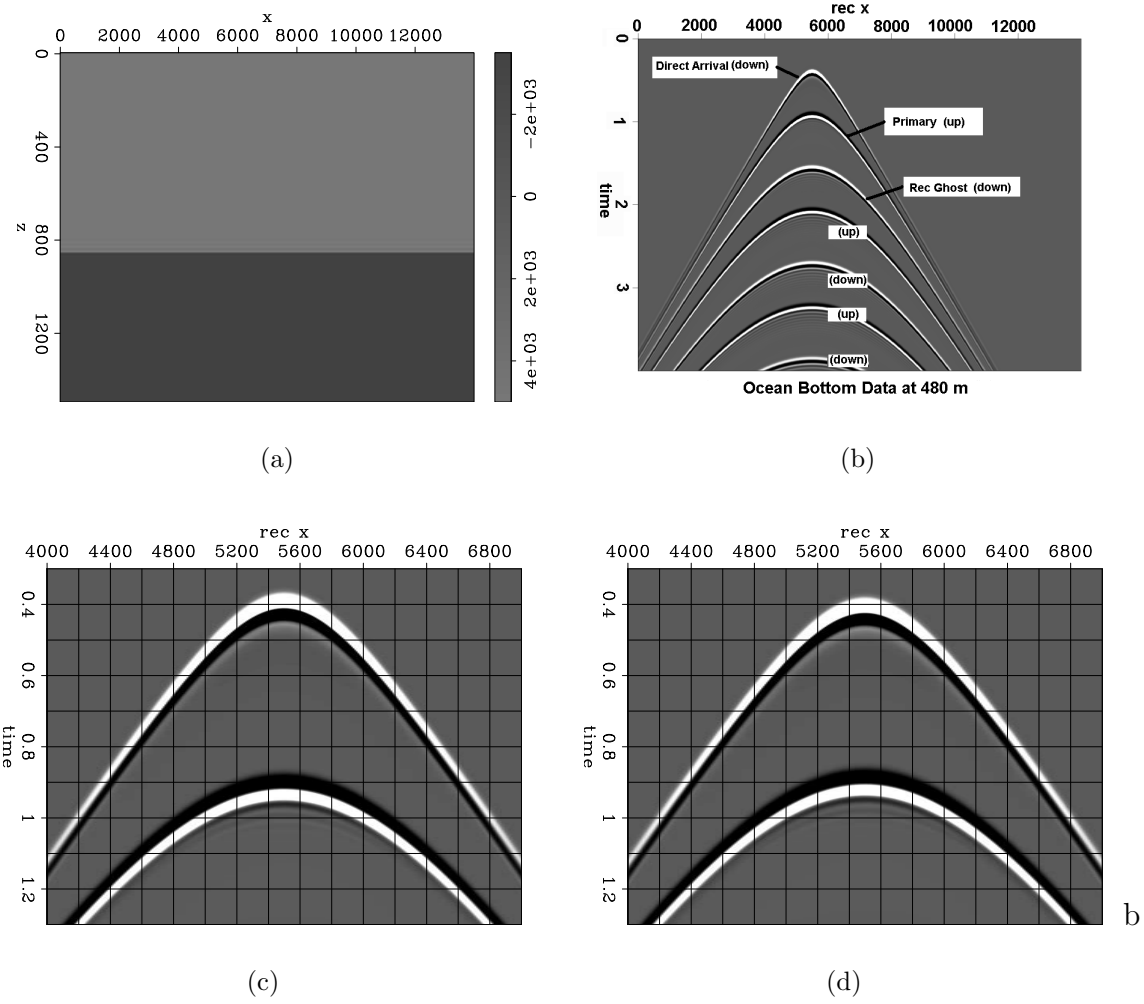

Figure 4: (a) Our simple one reflector velocity model. (b) The data collected at 480 m depth using the two-way acoustic wave equation. (c) The direct arrival and primary reflection of the over data. (d) The direct arrival and the primary reflection of the under data. **[CR]**

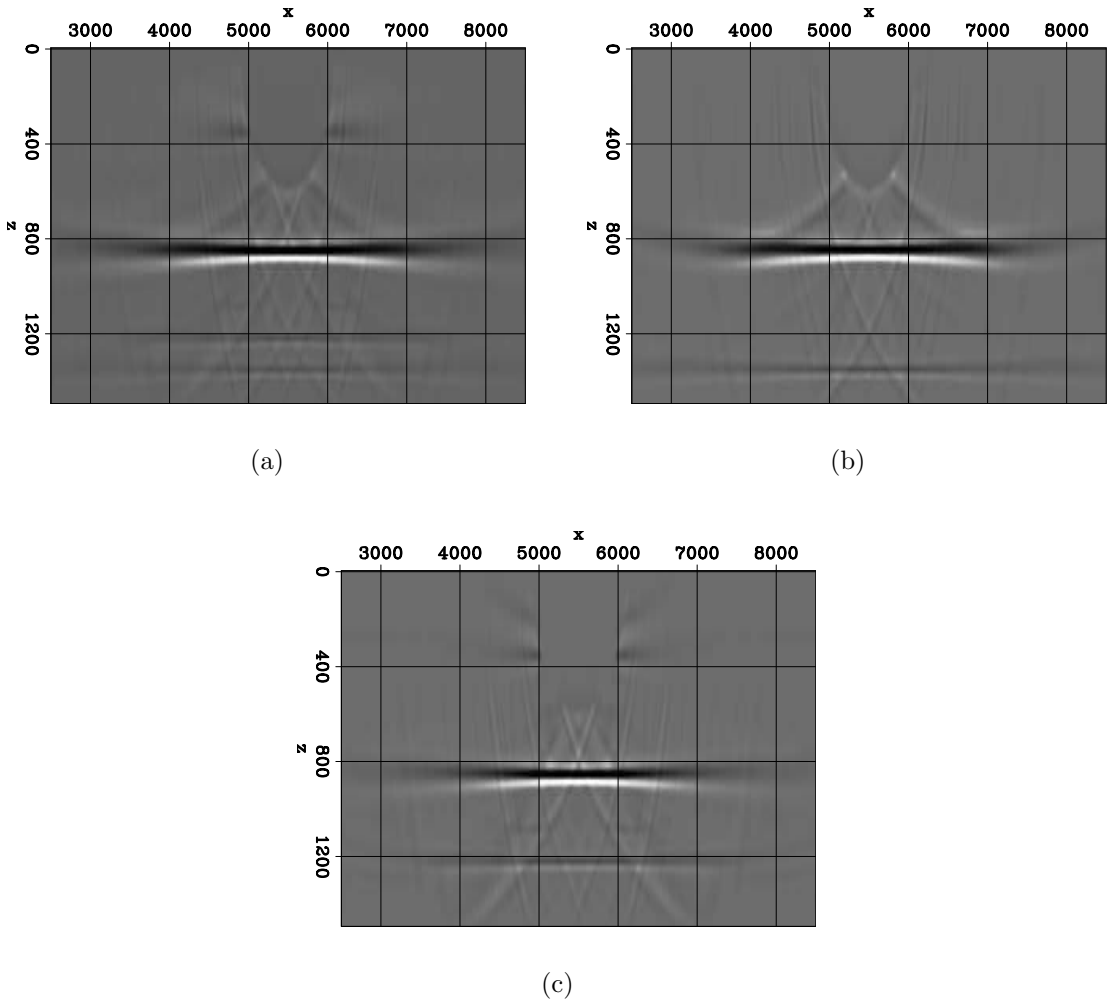

Figure 5: (a) The migration result using the over-under data. There is a reflector below the 800 m depth. In addition, there are also two weaker coherent artifacts at 1200 m and 1300 m depth. (b) The migration result of over-under with up-going only energy; (c) the migration result of over-under data with down-going only energy. **[CR]**

$$\begin{bmatrix} \tilde{d_o^{\uparrow}} \\ \tilde{d_u^{\uparrow}} \end{bmatrix} = \mathbf{S}' \left(\mathbf{S} \begin{bmatrix} d_o \\ d_u \end{bmatrix} \right)_{d_\downarrow = 0} = \mathbf{S}' \begin{bmatrix} d_\uparrow \\ d_\downarrow \end{bmatrix}_{d_\downarrow = 0}.$$

Note that the resulting data $\tilde{d_o^{\uparrow}}$ and $\tilde{d_u^{\uparrow}}$ are still in the over-under data space but contain only up-going energy. Similarly, to filter out the up-going energy in d_o and d_u, we can use:

$$\begin{bmatrix} \tilde{d_o^{\downarrow}} \\ \tilde{d_u^{\downarrow}} \end{bmatrix} = \mathbf{S}' \left(\mathbf{S} \begin{bmatrix} d_o \\ d_u \end{bmatrix} \right)_{d_\uparrow = 0} = \mathbf{S}' \begin{bmatrix} d_\uparrow \\ d_\downarrow \end{bmatrix}_{d_\uparrow = 0}.$$

The results of performing RTM with only the down-energy and only the up-energy are shown in Figure 5(b) and Figure 5(c) respectively. Both figures have the same clip. In Figure 5(b), the reflector at 800 m is much wider than the corresponding one in Figure 5(c). This is because migrating with down-going energy is primarily imaging with the receiver ghost signal. On the other hand, migrating with up-going energy is primarily imaging with the primary signal. Imaging with the receiver ghost data provides a wider subsurface illumination, because its point of reflection is further away from the receiver than that of the primary reflection. Another observation is that the amplitude of the 800 m reflector in figure 5(c) is stronger than the amplitude in Figure 5(b). The primary signal has stronger amplitude than any signal of higher order (ghost or multiples) because of geometric spreading. Therefore, imaging with the primary gives a higher-amplitude reflectivity model than imaging with the receiver ghost.

Artifacts in Ocean-Bottom RTM

The two artifacts that appear in Figure 5(a) can be identified when migrating with only up-energy and with only down-energy. The deeper artifact ($\approx$ 1300 m) appears in Figure 5(b) while the 1200 m artifact appears in figure 5(c). These artifacts do not appear in streamer RTM. When injecting the down-going data into the finite difference grid, the signal actually spreads both upward and downward in the computation grid. This creates spurious events when correlating, because down-going energy should only travel upward in reverse time. Similarly, up-going data should only traverse downward when injected in reverse time to the finite-difference grid. To alleviate this problem, we propose a joint inversion scheme. Such a scheme not only addresses the artifacts problem, it also provides a way to constructively combine up- and down-going migration results.

JOINT INVERSION OF UP-GOING AND DOWN-GOING OCEAN-BOTTOM DATA

The goals of our joint inversion scheme are threefold:

1. To migrate two of the four-component ocean-bottom data with acoustic modeling. Field data is collected as pressure (P)and vertical particle velocity (Z). To make use of the Z measurement, we would need to apply elastic modeling. Our proposed joint inversion scheme will avoid this difficulty.
2. To alleviate the migration artifacts in ocean-bottom RTM caused by to its acquisition geometry.
3. To combine up-going and down-going reflectivity solutions in a constructive way.

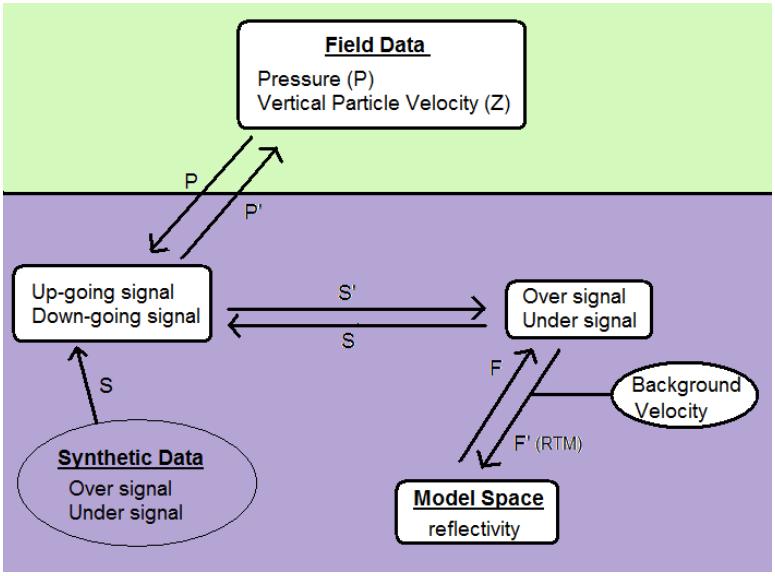

Figure 6: This flowchart shows the relationship between multi-component pressure (P) and vertical particle velocity (Z) data, up- and down-going data, and over/under data. Reverse time migration (RTM) is performed with over/undre data and generate reflectivity in migration using a background velocity model. [**NR**]

Our proposed scheme can be summarized using the flowchart in Figure 6. Field data d_P and d_Z can be converted into up-going and down-going data at the receiver level by applying the PZ summation operator $\mathbf{P}$. There are many ways to implement PZ summation; one of the simplest is described in Wong et al. (2009).

$$\begin{bmatrix} \tilde{d}_{\uparrow} \\ \tilde{d}_{\downarrow} \end{bmatrix} = \mathbf{P} \begin{bmatrix} d_P \\ d_Z \end{bmatrix}.$$

Next, up- and down-going data can be converted into over- and under- data using the adjoint of the separation operator $\mathbf{S}$:

$$\begin{bmatrix} \tilde{d}_o \\ \tilde{d}_u \end{bmatrix} = \mathbf{S}' \begin{bmatrix} \tilde{d}_\uparrow \\ \tilde{d}_\downarrow \end{bmatrix}.$$

RTM is performed using over and under data via the RTM operator, denoted as $\mathbf{F}'$:

$$\mathbf{m} = \mathbf{F}' \begin{bmatrix} \tilde{d}_o \\ \tilde{d}_u \end{bmatrix}.$$

Since all three operators are linear, we can do acoustic RTM on d_P and d_Z by applying a cascade of these operators, denoted as $\mathbf{L}'$:

$$\mathbf{m} = \mathbf{F}'\mathbf{S}'\mathbf{P} \begin{bmatrix} \tilde{d}_P \\ \tilde{d}_Z \end{bmatrix} = \mathbf{L}' \begin{bmatrix} \tilde{d}_P \\ \tilde{d}_Z \end{bmatrix}.$$

We claim that by applying the inverse operator $\mathbf{L}^{-1}$ instead of the adjoint operator $\mathbf{L}'$, the three goals discussed at the beginning of the section can be achieved. The testing of this theory is the focus of our current research.

CONCLUSION

We discuss our progress in migrating multi-component ocean-bottom data, focusing on joint inversion of up- and down-going data using two-way acoustic wave equation. We observe that applying RTM to up-going energy and down-going energy shows different illumination of the sub-surface. Migration of the up-going data gives strong reflector amplitude and weaker artifacts. However, its area of sub-surface illumination is narrower than migrating with the down-going signal due to mirror imaging. In addition, a new class of artifacts appears because of the injection of receiver wavefields with the ocean-bottom geometry. We propose a joint-inversion scheme that can constructively achieve three goals; (1) combining the up- and down-going migration result, (2) removing spurious artifacts in the final reflectivity model and (3) migrating multi-components ocean bottom data with only acoustic modeling.

ACKNOWLEDGMENTS

We also thank SeaBird Explorations for the release of the field dataset.

REFERENCES

Amundsen, L., 1993, Wavenumber-based filtering of marine point-source data: Geophysics, **58**, 1497–150.

Barr, F. J. and J. I. . Sanders, 1989, Attenuation of water-column multiples using pressure and velocity detectors in a water-bottom cable: 59th annual international meeting: SEG Expanded Abstracts, 653–656.

Baysal, E., D. Kosloff, and J. W. C. Sherwood, 1983, Reverse time migration: Geophysics, **48**, 1514–1524.

Dash, R., G. Spence, R. Hyndman, S. Grion, Y. Wang, and S. Ronen, 2009, Wide-area imaging from obs multiples: Geophysics, in press.

Ebrom, D., X. Li, and D. Sukup, 2000, Facilitating technologies for permanently instrucmented oil fields: The Leading Edge, **19**, 282–285.

Etgen, J. T., 1986, Prestack reverse time migration of shot profiles: SEP-Report, **50**, 151–170.

Sonneland, L., L. E. Berg, P. Eidsvig, A. Haugen, B. Fotland, and J. Vestby, 1986, 2-d deghosting using vertical receiver arrays: SEG Expanded Abstracts, **5**, 516.

White, J. E., 1965, Seismic waves: radiation, transmission, and attenuation: McGraw-Hill.

Whitmore, N. D., 1983, Iterative depth migration by backward time propagation: SEG Expanded Abstracts, **2**, 382.

Wong, M., B. L. Biondi, and S. Ronen, 2009, Joint inversion of up- and down-going ocean bottom data: SEP-Report, **138**, 225–234.

Yan, J. and P. Sava, 2008, Isotropic angle-domain elastic reverse-time migration: Geophysics, **73**, S229.